Non-contact infrared temperature measurements in dry permafrost boreholes

Ralf Junker,[1,2] Mikhail N. Grigoriev,[3] and Norbert Kaul[2]

Received 21 January 2007; revised 22 December 2007; accepted 23 January 2008; published 30 April 2008.

[1] While planning the COAST Expedition to the Siberian Laptev Sea in 2005, the question of how to make a short equilibrium temperature measurement in a dry borehole arose. As a result, an infrared borehole tool was developed and used in three dry boreholes (up to 60.2 m deep) in the coastal transition zone from terrestrial to sub-sea permafrost near Mamontovy Klyk in the western Laptev Sea. A depth versus temperature profile was acquired with equilibration times of 50×10^{-3} s at each depth interval. Comparison with a common resistor string revealed an offset due to limitations of accuracy of the infrared technique and the influence of the probe's massive steel housing. Therefore it was necessary to calibrate the infrared sensor with a high precision temperature logger in each borehole. The results of the temperature measurements show a highly dynamic transition zone with temperature gradients up to -0.092°C/m and heat flow of -218 mW/m. A period of submergence of only 600 years the drilled sub-sea permafrost is approaching the overlying seawater temperature at -1.61°C with a temperature gradient of 0.021°C/m and heat flow of 49 mW/m. Further offshore, 11 km from the coastline, a temperature gradient of 0.006°C/m and heat flow of 14 mW/m occur. Thus the sub-sea permafrost in the Mamontovy Klyk region has reached a critical temperature for the presence of interstitial ice. The aim of this article is to give a brief feasibility study of infrared downhole temperature measurements and to present experiences and results of its successful application.

Citation: Junker, R., M. N. Grigoriev, and N. Kaul (2008), Non-contact infrared temperature measurements in dry permafrost boreholes, *J. Geophys. Res.*, *113*, B04102, doi:10.1029/2007JB004946.

1. Introduction

[2] Technical solutions for measuring temperature via infrared radiation have been known since the 1920s. Devices used for measuring body temperature via radiation are called *pyrometers, infrared thermometers or radiation thermometers* [*Michalski et al.*, 2001]. These non-contact measurement techniques and can be divided in two groups: (1) manually operated pyrometers and (2) automatic pyrometers. The first needs human judgment to compare the object's color with a reference filament in the pyrometer and is exclusively suitable for very high temperatures. The second type is very promising as an application in Arctic dry boreholes because temperatures down to a limit of -50°C can be measured for which no change of a body's color due to temperature occurs. The concept and execution of measuring temperatures via infrared radiation in a borehole is a novelty because temperature dependent resistors (thermistors) and thermocouples are common and more recently the Distributed Temperature Sensing (DTS), which uses the Raman-Effect has been utilized [*Henninges et al.*, 2005]. The DTS has also been used in an air-filled borehole [*Macfarlane et al.*, 2002], but must overcome a long equilibration time and is more expensive than our device. Borehole temperatures provide information on temperature gradients and therefore on heat flow and paleo-climates [*Lunardini*, 1981; *Yershov*, 1998].

[3] In Arctic regions, the use of a drilling fluid is often not possible due to the extremely low temperatures or environmental regulations, and therefore scientists must cope with specialized borehole-data acquisition problems. For temperature measurements, it is generally difficult to couple the sensor with the borehole wall. In a borehole filled with fluid, the formation temperature can be determined by measuring the fluid temperature, because the thermal diffusivity of the fluid is sufficient to equilibrate with the surrounding rock in an adequately short time. In a dry borehole, air has a very low thermal diffusivity, and sensor equilibration to ambient temperature takes a long time unless the sensor directly touches the wall. *Diement* [1967] conducted laboratory experiments to determine the time necessary to equilibrate different types of thermistors in air to temperature changes. Depending on the design of the thermistors, it took 2000 to 5000 s. It was planned to measure temperature in several dry Arctic boreholes that were expected to be accessible for only several hours and therefore the speed of measurement was critical. To avoid

[1] GGA-Institut, Hannover, Germany.
[2] University of Bremen, FB5 Geosciences, Bremen, Germany.
[3] Permafrost Institute, Russian Academy of Sciences, Yakutsk, Yakutia, Russia.

0148-0227/08/2007JB004946$09.00

this problem, a borehole probe carrying an infrared temperature sensor (pyrometer) was designed and built to test a contact-free method of measuring temperature in dry boreholes by using the infrared radiation emitted by the surface of the borehole wall.

2. Physics of Infrared Temperature Measurement

[4] Every body with a temperature (T) above 0 K emits radiation within the infrared wavelength spectrum (between 0.7 to 1000 μm). This makes it possible to determine the temperature even of far distant objects. In astrophysics it is also used for the detection of cosmological radiation. Detecting infrared radiation requires no direct contact with the object, the influence of the air between the sensor and target is negligible, and measurements take on the order of 50×10^{-3} s. These features make infrared temperature measurements a promising application for temperature measurement in dry permafrost boreholes.

[5] The dependence of temperature on radiative intensity is non-linear and expressed by the Stefan-Boltzmann's law. The emitted energy (P) of a black radiator body varies with the temperature to the power of four as given in equation (1) (σ = *Stefan-Boltzmann constant*, A = *area*).

$$P = \sigma \cdot A \cdot T^4 \tag{1}$$

[6] The wavelength of maximum amplitude (λ) of infrared radiation shifts across the spectrum depending on the temperature (T in Kelvin) as described by the Wien displacement law (equation (2)).

$$\lambda_{\max} = \frac{2.89 \cdot 10^3 \mu\text{mK}}{T} \tag{2}$$

[7] Equation (1) is a simplification of the relationship between the energy of the infrared radiation and the temperature. The radiation from the surface of a real body consists of radiation due to its own temperature and a certain amount of radiation due to radiation reflected off, or transmitted through, the surface of the real body. A material-specific constant correction factor is required. The emission coefficient ϵ (equation (3)) takes account of this fact.

$$\epsilon = \epsilon_{emission} + \epsilon_{reflection} + \epsilon_{transmission} \tag{3}$$

[8] This leads to the complete equation (equation (4)) for the determination of the temperature of a real body.

$$P = \epsilon \cdot \sigma \cdot A \cdot T^4 \tag{4}$$

[9] A blackbody radiator has an emission coefficient ϵ of 1, which means the emitted infrared radiation truly represents the temperature of the body. Real bodies have $\epsilon \neq 1$, with ϵ varying from one material to the next. In solid bodies like rock and borehole casings no transmission occurs ($\epsilon_{transmission} = 0$) and due to the geometry of the borehole cavity internal reflections are absorbed ($\epsilon_{reflection} = 0$) thus $\epsilon \approx 1$ (equation (3)). If the depth of the borehole is at least six times the borehole diameter [*Michalski et al.*, 2001], the borehole wall can be assumed to emit blackbody radiation, and incident light (e.g., sunlight) doesn't impact the temperature measurements. Therefore in a borehole $\epsilon = 1$. Changes in material emissivity in the borehole wall may be ignored whether the borehole is open or cased.

3. Infrared Temperature Measurement Techniques

[10] The infrared borehole temperature measurement used an automatic pyrometer integrated in a borehole probe. Detector, signal converter and measuring instrument are integrated components of one autonomous device. The pyrometer itself is a commercial device (KT11) with a photoelectric detector manufactured by HEITRONICS in Wiesbaden, Germany (cylindrical design - total length: 150 mm (5.9″), diameter: 33 mm (1.3″)).

[11] For use in the Siberian Arctic, the pyrometer was specially enhanced to meet the requirements of such a harsh environment. To do so, all electronic components were tested to ensure they operated in a climate chamber at −30°C prior to assembly by HEITRONICS. The power supply and data cable had silicon insulation which, in contrast to PVC or rubber insulations, remains flexible at temperatures well below zero. The standard KT11 pyrometer was modified to operate at temperatures well below zero and had a measurement range from +25°C to −25°C. According to manufacturer, the absolute accuracy of the KT11 is given by

$$Error_{absolute} = \pm 1^\circ\text{C} + 0.1 \cdot \left(T_{sensor} - T_{target}\right) \tag{5}$$

with correctly adjusted emissivity in case of measuring a non blackbody radiator or a blackbody radiator with $\epsilon = 1$. The emissivity can be adjusted from 0.8 to 1.0 via a potentiometer inside the KT11 housing.

[12] In order to compare the KT11 IR-sensor to a standard logger, a laboratory test was conducted. The IR-sensor and a MTL (miniaturized data logger using a PT100 thermistor) [*Pfender and Villinger*, 2002] were simultaneously taken from room conditions (26.1°C) and placed into a PVC liner which simulated the borehole geometry of a black radiator. The liner was placed into a climate chamber at −14.3°C. The temperature in the chamber was also checked by a Fluke 16 Multimeter using a 80BK Integrated DMM Temperature Probe. The great advantage in equilibration time of the IR-sensor can clearly be seen in Figure 1.

[13] The HEITRONICS KT11 pyrometer is nearly cylindrical, with a length of 15 cm and a diameter of 3 cm. At one end is a cable connector while the other end has a recess with the infrared sensor. The pyrometer is built lengthwise into the probe. In order to be able to measure perpendicular to the borehole wall, a tilted mirror was attached to the sensor. The mirror was also manufactured by HEITRONICS and the KT11 had a factory-made calibration within a temperature range from 25°C to −25°C. Through an aperture in the probe body, the mirror reflects infrared radiation emitted by the borehole wall toward the detector. The diameter of the measuring field depends on the distance between the sensor and the borehole-wall and is smaller than 4.5 mm (Figure 2). A PVC-spacer mounted at the opening of the borehole probe prevented debris from falling into the radiation pathway. For downhole temperature

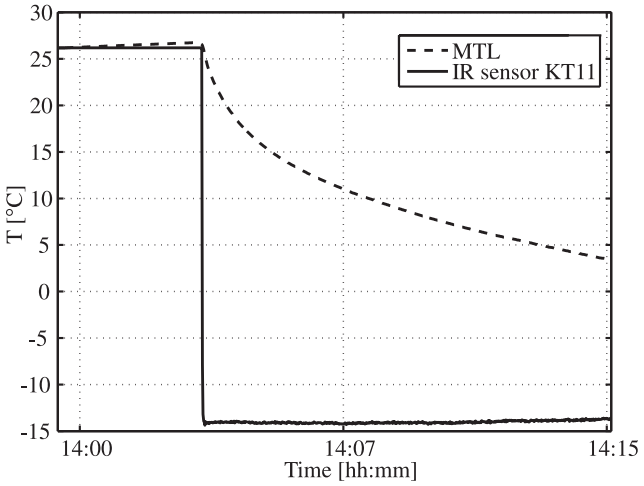

Figure 1. Temperature curves obtained from a laboratory experiment. This illustrates the speed of the KT11 infrared sensor compared to a MTL using a thermistor. Equilibration time of the IR-sensor was below the software sampling rate of one second. The KT11 and FLUKE 16 differ only by 0.2°C following equilibration at 14.1°C.

measurement the instrument needs to be connected to display equipment via a cable.

3.1. Coastal and Subsea Permafrost in the Siberian Laptev Sea

[14] The drilling sites where the infrared borehole probe was to be tested are located in the coastal area of the western Laptev Sea in Siberia called Mamontovy Klyk (mammoth tusk, Figure 3). The test was conducted during a German Ministry of Education and Research funded (*Bundesministerium fr Bildung und Forschung*) coastal drilling expedition COAST, carried out by scientists from the Alfred Wegener Institute for Polar and Marine Research (*AWI*), Permafrost Institute Yakutsk *PIY, Yakutsk*), Arctic- Antarctic Research Institute (*AARI*, *St. Petersburg*) and the University of Bremen. One objective of the expedition COAST was the acquisition of temperature data in the transition zone from terrestrial to submarine permafrost (Figure 4).

[15] Most of the Laptev Sea (Figure 3) and adjacent hinterland remained unglaciated during the last glacial maximum. As a result, permafrost developed down to depth as great as 1000 m. Today, mean annual air temperatures are approximately −11 to −12°C [*Dereviagin and Kunitsky*, 2004] with seasonal variations reaching from −45°C in winter up to +20°C in July. The land surface is characterized by polygonal patterned ground, which is typical for Arctic regions. The polygons have a diameter of some 10s of meters and the edges are underlain by ice-wedges that penetrate the peaty and sandy soil. After thousands of years of growth, the ice-wedges near Mamontovy Klyk have merged to form most of the ground and can be seen in the coastal cliff as ice complexes [*Romanovskii et al.*, 2000; *Schirrmeister et al.*, 2002]. Sediments in this area are known to be mostly sandy with partly silty sections and ice contents of >80% by volume [*Rachold et al.*, 2007]. Further physical rock properties are subject to ongoing examinations.

[16] As the coastal regions of the Laptev Sea experience high rates of coastal retreat (up to 15 m/a in some areas) terrestrial permafrost is submerged and exposed to the thermal and chemical influence of saline and relatively

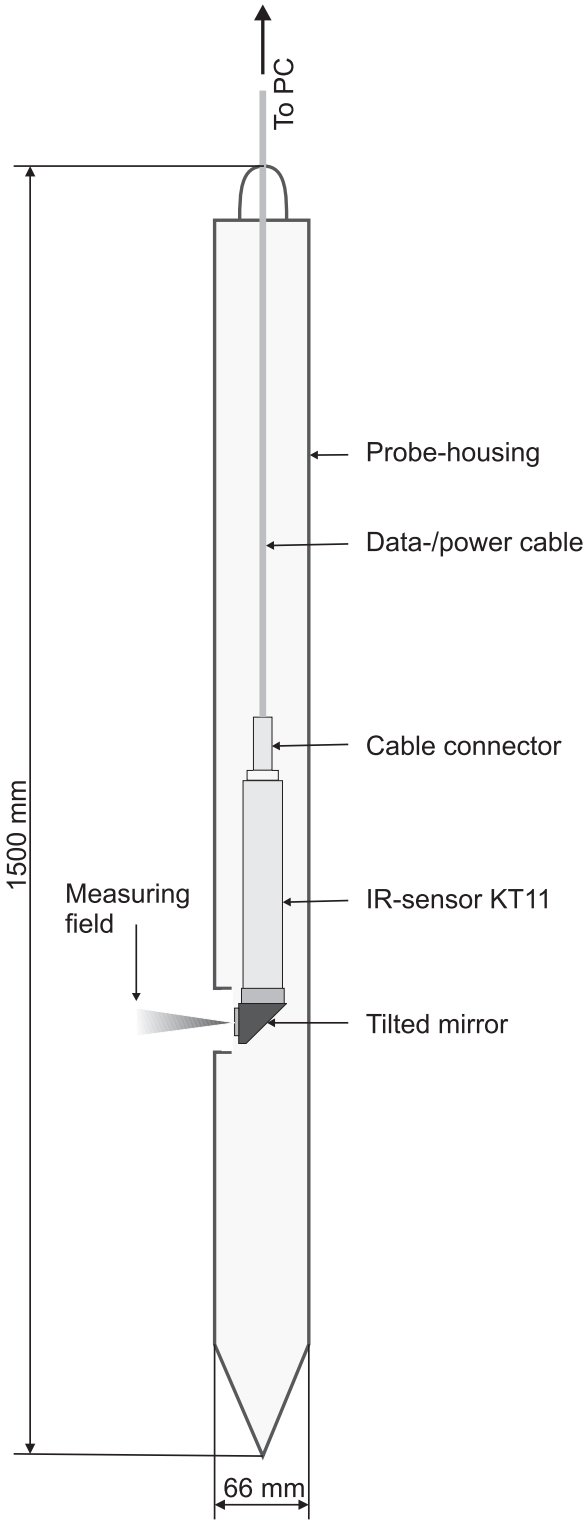

Figure 2. The schematic design of the infrared borehole tool showing the implementation of the IR sensor within the probe. The overall weight is 15 kg, mostly due to the stainless steel housing.

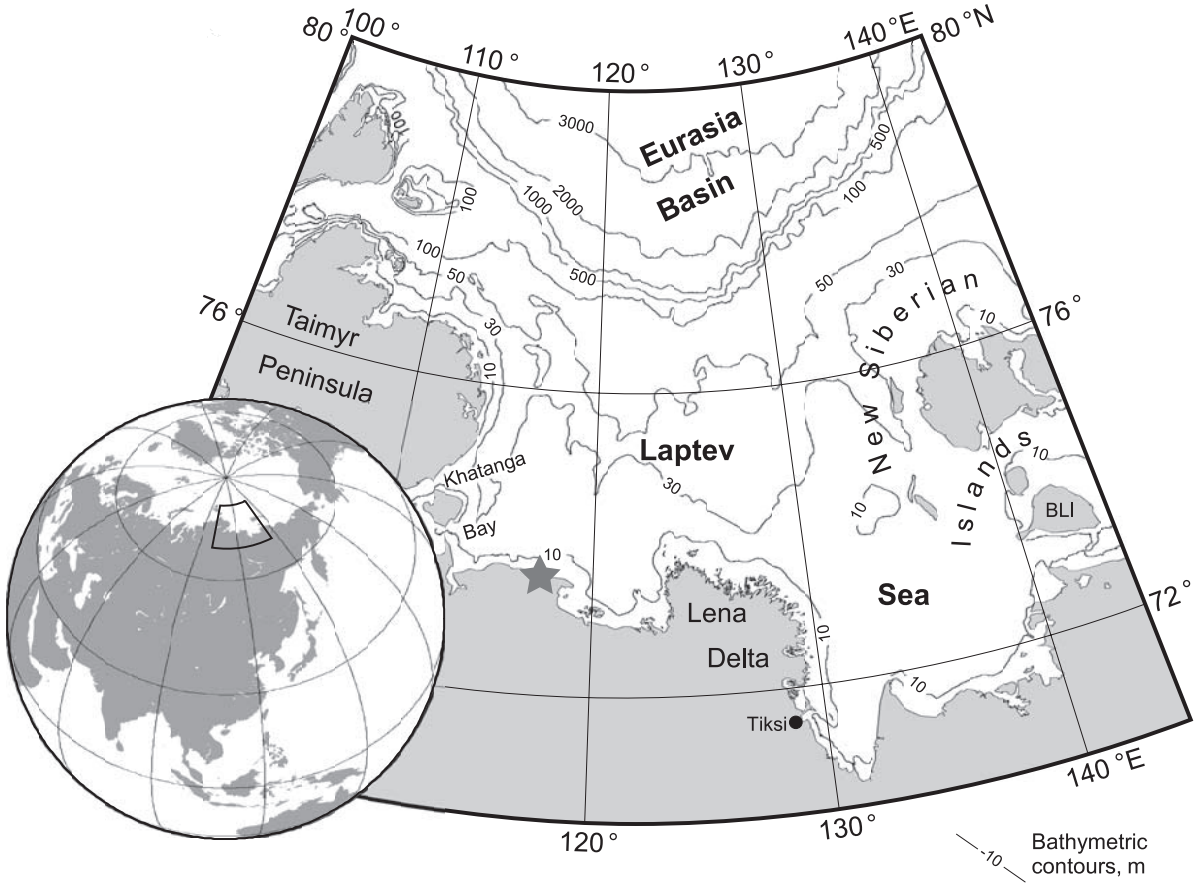

Figure 3. The Siberian Laptev Sea from the Taimyr Peninsula in the west to the New Siberian Islands and Great Lyakovsky Island (BLI) in the east. With an extent of 670,000 m^2, the Laptev Sea is one of the epicontinental seas of the Arctic Ocean. Water depths throughout most of the Laptev Sea are less than 50 m. The terrestrial drilling location at Mamontovy Klyk is marked with a star.

warm (average −1.5°C) Arctic seawater. For this reason the subsea permafrost is degrading steadily. On the basis of modeling and interpretation of geophysical data, this ''relic permafrost'' or so-called subsea permafrost [*Osterkamp*, 2001] is believed to underlie most of the Laptev Sea Shelf down to a water depth of approximately 100 m [*Rachold et al.*, 2007].

[17] Temperature measurements acquired during COAST expedition can provide evidence for the existence, extension and thermal state of the subsea permafrost in the coastal region of the Laptev Sea. The coastal transition zone from terrestrial to subsea permafrost in particular is a key region for understanding the evolution of subsea permafrost [*Rachold et al.*, 2007].

[18] The onshore drilling site C1 was set approximately 110 m inland from the shoreline. This borehole was drilled at the center of a polygon in order to core sediments rather than ice. The final depth was planned to be 60 m and after a drilling time of 36 h the borehole was terminated at 60.2 m. An 11-day thermal equilibration period occurred between the cessation of drilling and the final temperature measurement of C1. Thereafter, in chronological order, the boreholes C2, C3, C4, and C5 were drilled into the sea bottom from the sea-ice surface (Figure 5).

[19] The most suitable season for drilling the subsea permafrost is spring-time, since ambient temperatures are warm enough to work outside, but still cold enough to assure stability of the sea ice. In summer, the average water depth in the coastal areas of the Laptev Sea barely exceeds 3 to 6 m. Therefore this region is not accessible by water-bound drilling vessels in the warm seasons. All boreholes on the transect during COAST expedition have been drilled by a Russian type mobile drill rig (URB-2A-2) on skids with a hydraulic rotary-pressure mechanism. No drilling fluid was used. In order to retrieve material from the well, a core bit with a core retainer was used. Well tubes and bore casings from 1.5 to 4.0 m length with diameter $5\frac{7}{8}''$ (147 mm), $5''$ (125 mm), $4\frac{1}{4}''$ (108 mm) and $3\frac{5}{6}''$ (89 mm) were used during drilling and prevented seawater from entering the borehole, protruding some 80 cm above the ground or ice surface. Consequently, all boreholes were planned to be dry, because seawater flowing into the well would disturb the temperature and could possibly freeze and thus make the bore inaccessible for measurement tools.

[20] *Lachenbruch et al.* [1982] published an analytical approximation of the disturbance of the temperature caused by the drilling process. In this context, *Lachenbruch and Brewer* [1959], *Lachenbruch et al.* [1982] and *Bullard* [1947] assume the borehole filled with circulating drilling

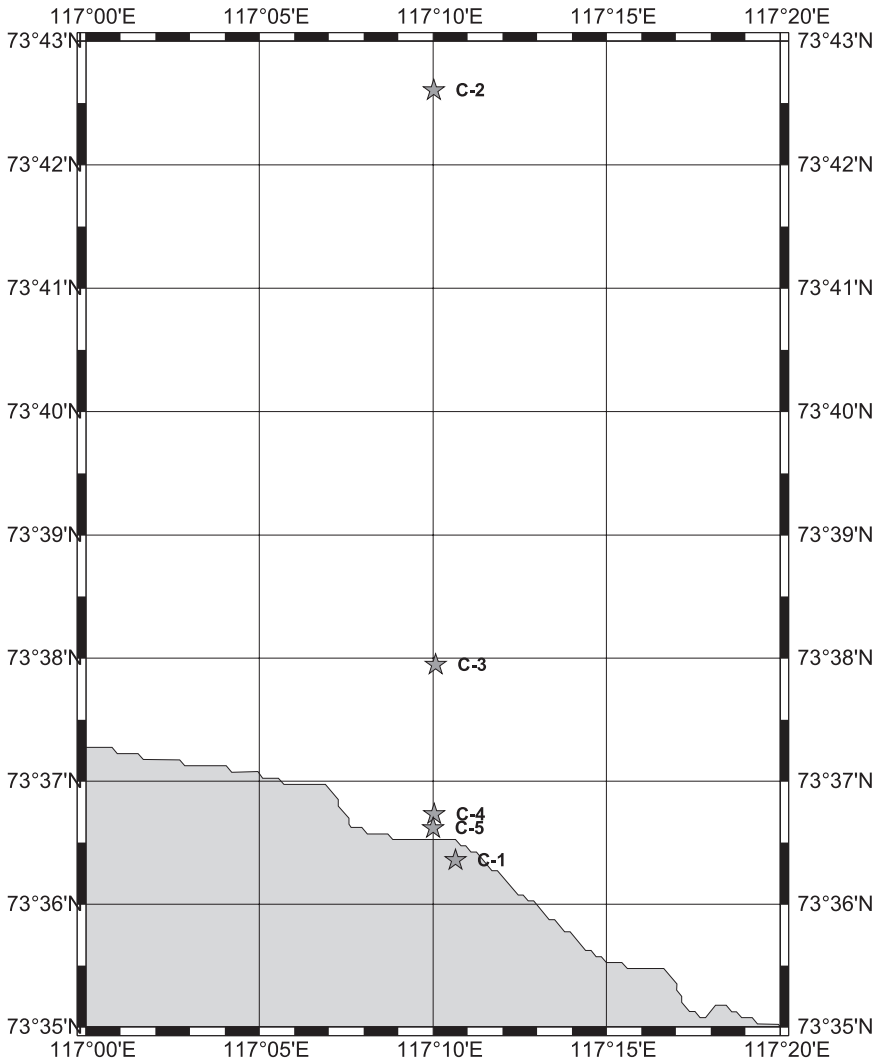

Figure 4. Locations of the boreholes C1 to C5 at Mamontovy Klyk.

fluid acts as a line source for heat which elongates during drilling and acts as a constant temperature boundary. In the case of Mamontovy Klyk no drilling fluid was used. Thus several orders of magnitude less heat was applied to the borehole wall than during conventional drilling. The air-filled borehole's thermal conductivity and heat capacity are also several magnitudes less than of the surrounding rock. Since no circulation in the borehole took place, it is more likely that temperature disturbance derives from the frictional heating of the drill bit and cooling from the drill pipes from the cold surface after disassembling. Neither process was quantified during the COAST expedition, but the frictional heat has a much smaller effect on the formation temperature of the formation than drilling fluid would have [*Bullard*, 1947]. Therefore the equation of *Lachenbruch et al.* [1982] can not deliver applicable information about the thermal equilibration of the boreholes. Furthermore, in the examples given by *Lachenbruch et al.* [1982] the temperature profiles diverge toward the top because this part has been under influence of the drilling fluid for the longest period. Successive measurements in C1 do not show this phenomenon. In the case of borehole C1, with an equilibration time of 11 days and a drilling time of one and a half days, borehole temperatures should have been quite close to the normal formation temperature. In the case of boreholes C4 and C5, the relaxation time after drilling was just one or two days. Because of the expedition's schedule to return to Tixi before break-up of sea and river ice, however, no more time could be spent on equilibration.

3.2. Measurement With IR-Probe

[21] The IR-probe could be used only in boreholes C1, C3, and C5. Borehole C2 was strongly twisted by the tidal movements of sea ice so that the probe got stuck in the first few meters. C4 was flooded soon after completion due to a leak in the casing. All of the boreholes could be measured by the thermistor string.

[22] The IR-temperature probe was used in the manner of a wireline logging tool (Figure 6). For measurement, the necessary equipment consisted of a tripod with a manually operated winch to lower the tool down the borehole, a 4 mm steel cable connected to the winch carried the probe, a highly flexible seven-wire silicon cable (70 m) for data

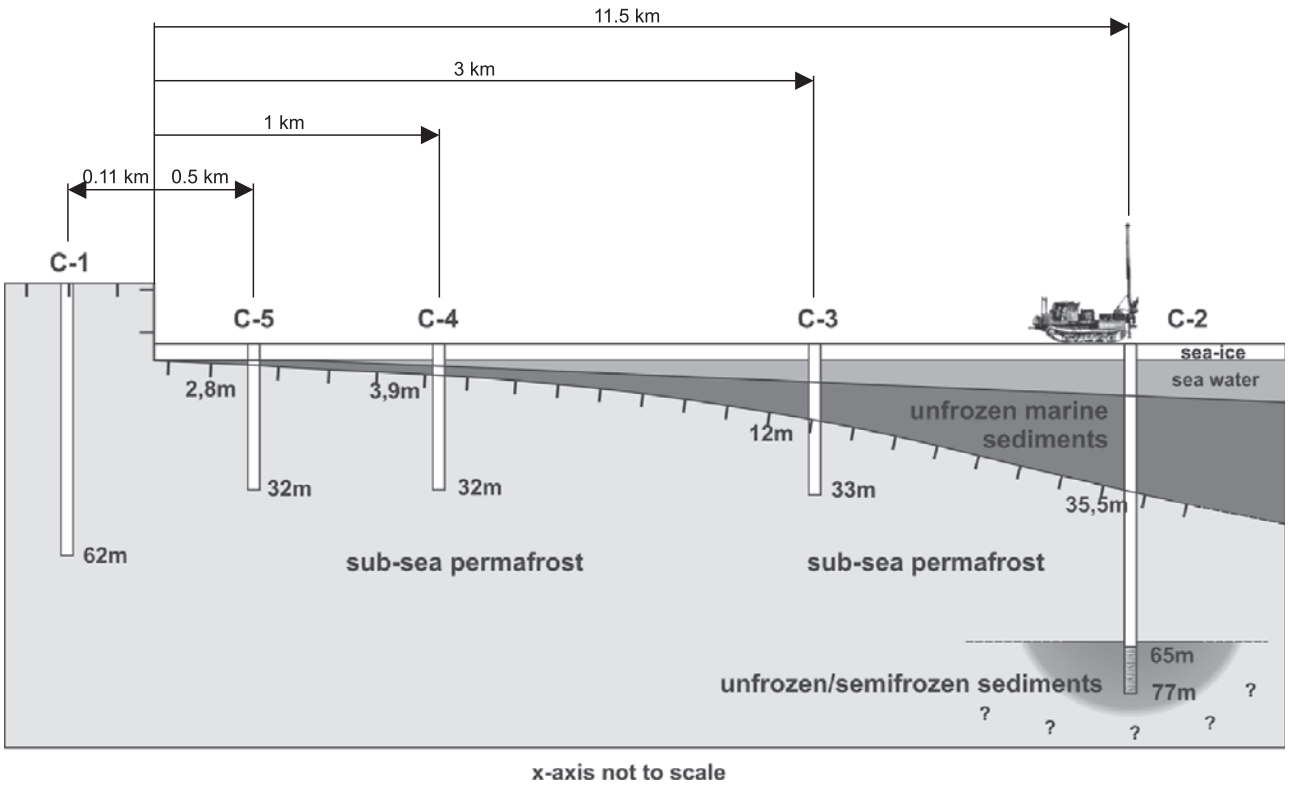

Figure 5. Cross-section of the drilling sites. The permafrost table was found in all offshore boreholes, whereas the young sedimentary marine cover increased with distance from shore. A special feature was found in borehole C2 where unfrozen marine sediments of Eemian age were found below the subsea permafrost [*Rachold et al.*, 2007].

communication and a display device connected to a laptop via RS232. In order to prevent hazardous high voltage pulses from the generator, the infrared detector was powered by a 24 volt battery.

[23] The display device (M35 from HEITRONICS) provided real-time temperature data to the computer. A short script was written in MATLAB to read the data automatically and save it to hard disk. Information on sensor depth was acquired manually. During the total measurement of the borehole, the IR-probe was recording temperature data every second. After stopping the probe at the measurement depth for at least 10 s the data for that depth was noted on the M35. A counter attached to the winch showed the current depth of the infrared probe. To correlate time/temperature data from the tool with the time/depth data from the winch, the tool was lowered to the next measuring depth within 20 s and depth and time were noted. Temperature/depth data pairs were correlated after measurement. Because of the experimental state of this method it was not possible to conduct a continuous automatic measurement. For future measurements this certainly needs to be improved in order to utilize the full potential of the tool.

[24] According to manufacturer instructions, the infrared probe needed to be switched on for at least 5 min prior to measurement in order to eliminate an initial drift of the infrared detector. Two people were required: one to operate the winch and the other to lower and to lift the data cable, since it could not be wound up by the winch. With all the safety precautions of a initial deployment, it took approximately 15 min to obtain 17 temperature measurements in the 60-m-deep borehole C1.

[25] Temperature was also measured with a thermistor string and with a high precision miniaturized temperature data logger (MTL) with an accuracy of ±5 mK that was manufactured by ANTARES Umwelt- und Geotechnik [*Pfender and Villinger*, 2002]. The data generated served to corroborate the infrared temperature probe data. The MTL is a cylindrical low-weight autonomous data logger (16 cm long, 15 mm in diameter), which was lowered to the bottom of the well where the sensor had direct contact with the rock and remained there for 15 min. In case of borehole C1 on April 25th, this provided a precise temperature of -12.49°C at the bottom of the borehole value used later in calibrating the temperature acquired by the IR-probe (Figure 7). The thermistor string was used to obtain temperature data for comparison at distinct depths in the well. It was deployed in the well for one to two hours until the resistivity readings were stable within resolution.

[26] Measurements with the thermistor string and the MTL were taken before the use of the infrared probe, because lowering and lifting of the probe would disturb the layering of the air in the borehole and therefore distort the result. Relaxation time for the MTL was about 15 min with direct contact to the bottom of the boreholes. Final temperature was derived from manual resistance measure-

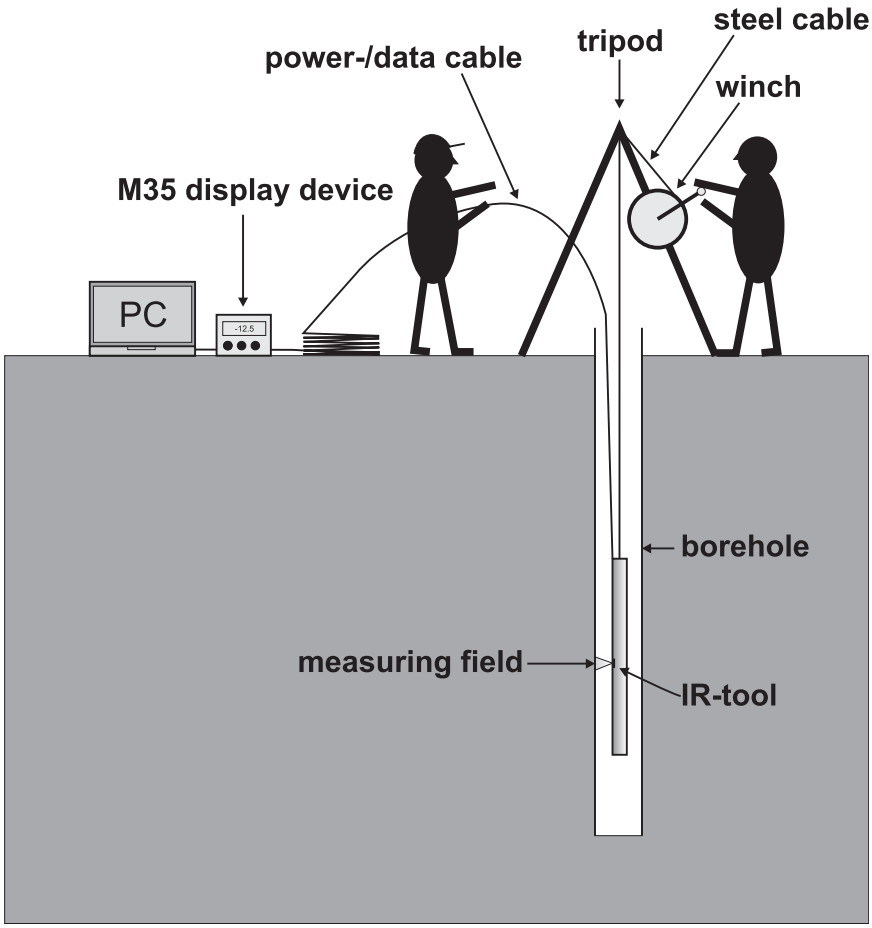

Figure 6. Sketch of the wireline downhole temperature measurements using the infrared temperature probe. The tool, which is attached to a steel cable, is lowered into the borehole via a winch mounted to a tripod.

ments of the respective thermistors using a digital ohmmeter and conversion table.

4. Results

[27] We first show the temperature measurements taken in C1 because more data have been acquired with which to judge the IR-probe. The results of all measurements taken in borehole C1 at Mamontovy Klyk are given in Figure 7, which shows data acquired with the resistor string and data obtained by the IR-probe.

[28] The upper three meters have greatly differing initial temperatures. This is a result of changes in ambient air temperature and the intensity of incident solar radiation on the protruding part of the casing during the first measurement on April 14th to April 25th. Altogether, the temperature-data show the winter signal propagating downward into the soil. The curves show a more or less sudden drop in temperature within the uppermost three meters, since the measurements were taken in late spring-time and much lower winter temperatures were still preserved lower in the hole. Then, temperatures rose again to a maximum between 10 to 11 m depth, which represents the prograding temperature signal of the previous summer. Below a depth of approx. 20 m, seasonal temperature variations are damped and the ground temperature approaches the mean annual temperature of −12°C [*Dereviagin and Kunitsky*, 2004].

[29] Each set in Figure 7 shows variations between measurements. The shift in the resistor string data toward lower temperatures results from the relaxation of thermal disturbance after the drilling process, whereas the ir-probe shows temperatures shifting in the opposite sense. A distinct offset exists between corresponding measurements of the thermistor string and the infrared-probe. The offset was observed in the field use for the first time. The average deviation between the string and the IR-probe was 0.35°C on the 14th, 1.18°C on the 21st and 1.56°C on the 25th. The upper 5 m were not considered due to the influences of solar radiation and ambient air temperature.

[30] Traditional methods for temperature measurement, such as thermistors and thermocouples, have been proven to provide excellent data given appropriate time for equilibration with the target. The prototype infrared temperature probe provides a non-contact alternative that can provide rapid measurements, but a temperature offset from the thermistor string was evident in the field deployment. It is unlikely that changes in borehole emissivity result in the observed discrepancy because the ratio of the borehole depth to its diameter is large. As mentioned in section 2 for a geometric configuration like a borehole, which is more

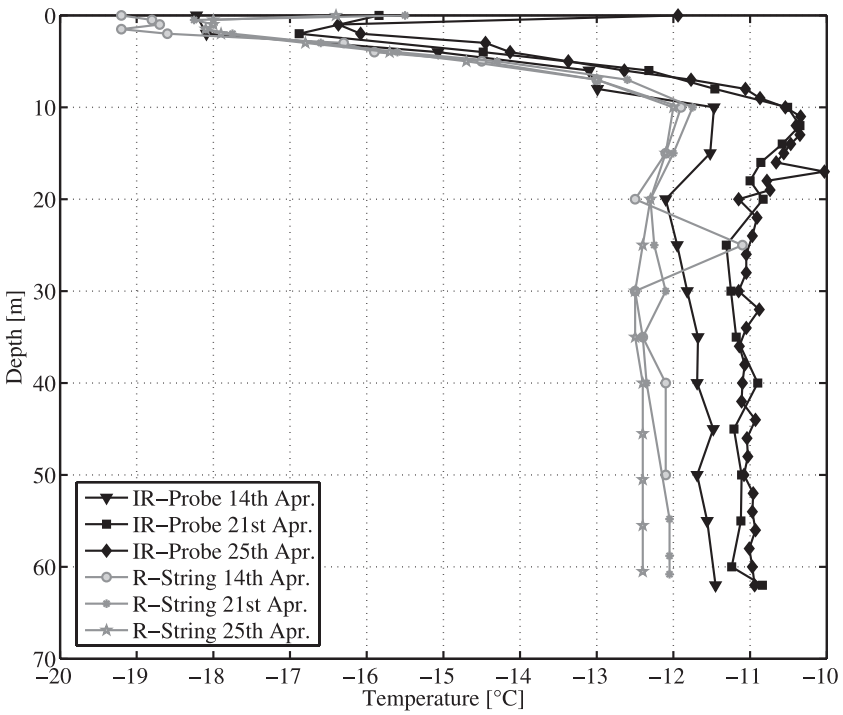

Figure 7. Temperature measurements taken in borehole C1 using the resistor string and the IR-probe. Seasonal temperature variations are faint at depths below 20 m and show the average mean annual temperature. There is a distinct offset between the curves due to the different methods of measurement and the thermal relaxation after the drilling process. However, the temperature trend with increasing depth is common to both temperature profiles.

than six times deeper than its diameter, the cavity acts like a blackbody radiator and emissivity becomes 1, no matter what type of rock or casing occurs. In contrast, laboratory tests run without the probe's 15 kg steel housing did not show this offset. In the case of the measurements taken at Mamontovy Klyk, solar irradiation and ambient temperature at the surface differed with each measurement, meaning the probe housing temperature also differed with each measurement. As shown in Figure 7, the apparent borehole temperature increases with increasing surface temperature, suggesting that the probe housing's thermal mass influences either the borehole wall temperature, or the measurement of the wall temperature.

[31] For this reason, an on-site calibration was necessary. To do so, the difference of the temperature measured by the ir-tool and the MTL at the bottom of the borehole was subtracted from the ir-data as an offset. This was done repeatedly for each hole and each run. After the temperature calibration was applied to the infrared data the mean average deviation of the complete borehole compared with the thermistor string could be reduced to -0.042°C in C1. This correction is important for temperature measurements but has no impact on the temperature gradients calculated from the IR-data.

[32] Looking at the temperature and temperature gradients from all boreholes (Figure 8) of the coastal transect in the Mamontovy Klyk area gives a clear idea of the thermal state of the sub-sea permafrost (Figure 8 and Table 1). C1 represent the thermal condition of the terrestrial permafrost in the coastal region. The temperatures in C5 and C4 indicate a gradual shift toward marine boundary conditions. These are highly dynamic areas, where seawater temperatures rise well above 0°C in summer, and where (C5) the sea ice touches the sea bottom in winter, so that they experience high temperature gradients of -0.062 to -0.092°C/m. Boreholes C2 and C3 show almost constant temperatures with very low positive temperature gradients of 0.006 to 0.008°C/m (Table 1). First results of ongoing core measurements show an average thermal conductivity of the frozen sections of C1 at -15°C of $2.37\frac{W}{m \cdot K}$ [*Overduin*, pers. comm.]. The data have been provided courtesy of Alfred Wegener Institut in Potsdam and the Geoforschungzentrum Potsdam. Measurements have been taken by using a TK04 manufactured by TEKA. Assuming from the observations of the cores retrieved that sediments in boreholes C2 to C5 are similar to C5, and that the thermal properties are the same, heat flow for all drilling locations can be calculated (Table 2).

[33] Sub-sea permafrost was found in cores from all boreholes below the marine sedimentary cover [*Rachold et al.*, 2007]. A special feature was found in borehole C2 where unfrozen sediments occurred below 64.7 meters below sealevel, which were unfrozen even at negative temperatures of about -1.5°C due to pore water salinity [*Rachold et al.*, 2007]. Further detailed data on lithology and salinity have been published by *Rachold et al.* [2007]. Measured borehole temperatures, temperature decay with time of submergence and temperature gradients, leads us to question models predicting a subsea permafrost thickness of

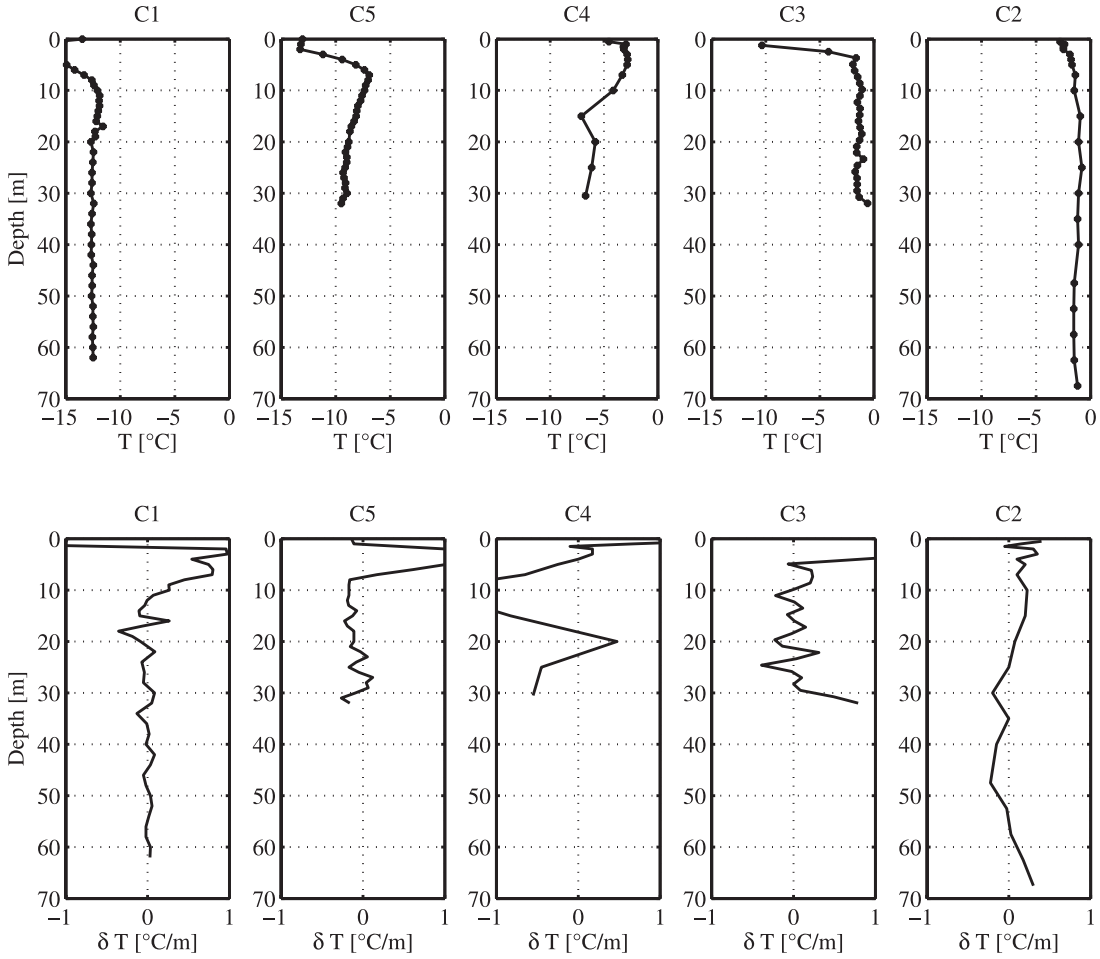

Figure 8. Temperatures (upper row) and temperature gradients between adjacent measurements (lower row) of boreholes C1 to C5. Data from C1, C3 and C5 have been acquired by the IR-probe. Boreholes C2 and C4 were measured by a thermistor string.

more than 400 m across most of the Laptev shelf. However, if the stability conditions for subsea permafrost are critical even in the "cold and young" coastal areas far from riverine warm water intake it is likely that the relic subsea permafrost may have already degraded completely in many places under the shelf.

[34] Assuming the present rate of coastal retreat of 5 m/a [*Grigoriev, M.*, *N.* pers. comm.] in the Mamontovy Klyk area has been constant during the Holocene, it is possible to estimate the thermal decay of the subsea permafrost. Given a 5 m/a coastal retreat rate, the furthermost borehole from the shore, C2, was submerged approx. 2300 years b.p. The locations of C3 and C4 were flooded 600 and 200 years b.p. respectively, and C5 was submerged some 100 years ago.

[35] Summarizing all the results acquired by the IR-temperature measurements, the following statements can be made: The submerged terrestrial permafrost, now subsea permafrost, is experiencing drastic thermal change. A highly dynamic area, explored by boreholes C4 and C5, is exposed to conditions in which sea ice touches the sea bottom during winter, but heating up of extremely shallow water results in non-trivial sea bottom heat fluxes in the summer. Boreholes C2 and C3 did not experience significant thermal changes during the recent geological past. The extremely low temperature gradients of some 0.008° C/m and low heat flow of 14 $\frac{mW}{m^2}$ show there is almost no heat flux. This can only occur if all the heat is consumed as latent heat of fusion due to the melting and degradation of subsea permafrost in the Mamontovy Klyk area. Additionally the presence of salt

Table 1. Boreholes Drilled During COAST Expedition

Borehole	Latitude	Longitude	Depth	Dist. to Coast	Equ.-Time	IR-Probe	Thermistor
C1	N 73° 36′ 21.5″	E 117° 10′ 38.5″	60.2 m	0.11 km	0/7/11 days	Yes	Yes
C2	N 73° 42′ 36.1″	E 117° 10′ 01.1″	77.0 m	11.5 km	7 days	No	Yes
C3	N 73° 37′ 56.8″	E 117° 10′ 04.4″	33.3 m	3.0 km	6 days	Yes	Yes
C4	N 73° 36′ 43.9″	E 117° 10′ 02.1″	32.1 m	1.0 km	4 days	No	Yes
C5	N 73° 36′ 37.0″	E 117° 09′ 59.8″	32.5 m	0.5 km	1 days	Yes	Yes

Table 2. Thermal Properties of Boreholes

Borehole	Distance to Coast	Bottom Water Temperature	Bottom Hole Temperature	Average Gradient	Heatflow
C1	0.11 km	···	−12.49°C	−0.008°C/m	$-19\ \frac{mW}{m^2}$
C2	11.5 km	−1.54°C	−0.89°C	0.006°C/m	$14\ \frac{mW}{m^2}$
C3	3.0 km	−1.61°C	−0.58°C	0.021°C/m	$49\ \frac{mW}{m^2}$
C4	1.0 km	−1.67°C	−7.02°C	−0.092°C/m	$-218\ \frac{mW}{m^2}$
C5	0.5 km	−7.01°C	−9.45°C	−0.062°C/m	$-147\ \frac{mW}{m^2}$

from the infiltration of seawater into the permafrost and the presence of salty marine sediment depressing the freezing point boosts the degradation [*Rachold et al.*, 2007].

5. Conclusions

[36] The temperature data acquired by the IR-probe contributed to new insights of the present state of the subsea permafrost in the coastal area of the Mamontovy Klyk region in the western Laptev Sea. Initially it seemed to be necessary to design a heavy probe to facilitate its movement down the borehole. During the deployment, probe mobility was only a problem in the deviated borehole C2. We therefore believe, that the IR-probe can be made more accurate by using a different housing. A PVC- rather than a steel housing should reduce the housing's influence on the measurements. In locations where measurements are hampered by low thermal conductivity media such as air and for which the cavity geometry provides blackbody behavior, such as in a borehole, the infrared non-contact technique is a quick, reliable and affordable alternative to common temperature measurement technique.

[37] **Acknowledgments.** I would like to express my gratitude to the following people: Volker Rachold, Waldemar Schneider, Viktor V. Kunitzky and Dimitry Y. Bolshyanov who made the COAST an expedition both enjoyable and successful. Furthermore I thank Heinrich Villinger, Paul Overduin, Peter Clift and Martin Heeseman for their scientific and technical support and thanks to the BMBF (project number: 03G0589D) and to the AWI for funding this project.

References

Bullard, E. C. (1947), The time necessary for a borehole to attain temperature equilibrium, Monthly Notices of the Royal Astronomical Society, *Geophys. Suppl.*, *5*(5), 127–130.

Dereviagin, A., and V. Kunitsky (2004), Russian-German cooperation SYSTEM LAPTEV SEA: The Expedition Lena-Anabar 2003, in *Reports on Polar- and Marine Research*, vol. 489, pp. 63–66, Boehl & Oppermann GmbH in Bremerhaven, Germany.

Diement, W. H. (1967), Thermal regime of a large diameter borehole: Instability of the water column and comparison of air- and water-filled conditions, *Geophysics*, *32*(4), 720–726.

Henninges, J., J. Schroetter, K. Erbas, and E. Huenges (2005), Temperature field of the Mallik gas hydrate occurrence - Implications on phase changes and thermal properties, in *Scientific Results from the Mallik 2002 Gas Hydrate Production Research Well Program, Mackenzie Delta, Northwest Territories, Canada*, edited by S. R. Dalimore and T. S. Collett, Geological Survey of Canada Bulletin *585*.

Lachenbruch, A. H., and M. C. Brewer (1959), Dissipation of the temperature effect of drilling a well in Arctic Alaska, experimental and theoretical geophysics, *Geol. Surv. Bull.*, *1083-C*, 73–109.

Lachenbruch, A. H., J. H. Sass, B. V. Marshall, and T. H. Moses Jr. (1982), Permafrost, heat flow, and the geothermal regime at Prudhoe Bay, Alaska, *J. Geophys. Res.*, *87*(B11), 9301–9316.

Lunardini, V. J. (1981), *Heat Transfer in Cold Climates*, John Wiley & Sons Inc., Hoboken, NJ, U.S.A.

Macfarlane, P. A., A. Foerster, D. F. Merriam, J. Schroetter, and J. M. Healey (2002), Monitoring artificially stimulated fluid movement in the Cretaceous Dakota aquifer, western Kansas, *Hydrogeol. J.*, *10*(6), 662–673.

Michalski, L., K. Eckersdorf, and J. McGhee (2001), *Temperature Measurement*, 2nd ed., 501 pp., John Wiley & Sons Ltd., Chichester.

Osterkamp, T. E. (2001), *Subsea Permafrost, Encyclopedia of Ocean Sciences*, edited by J. H. Steele et al., pp. 2902–2912, Elsevier, New York.

Pfender, M., and H. Villinger (2002), Miniaturized data loggers for deep sea sediment temperature gradient measurements, *Mar. Geol.*, *186*, 557–570.

Rachold, V., D. Y. Bolshiyanov, M. N. Grigoriev, H.-W. Hubberten, R. Junker, V. V. Kunitsky, F. Merker, P. Overduin, and W. Schneider (2007), Nearshore Arctic subsea permafrost in transition, EOS *88*(13), 149–156.

Romanovskii, N. N., A. V. Gavrilov, V. E. Tumskoy, A. L. Kholodov, C. Siegert, H.-W. Hubberten, and A. V. Sher (2000), Environmental evolution in the Laptev Sea region during late Pleistocene and Holocene, *Polarforschung*, *68*, 237–245.

Schirrmeister, L., C. Siegert, V. V. Kunitzky, P. M. Grootes, and H. Erlenkeuser (2002), Late Quaternary ice-rich permafrost sequences as a paleoenvironmental archive for the Laptev Sea region in northern Siberia, *Int. J. Earth Sci.*, *91*, 154–167.

Yershov, E. D. (1998), General geocryology, Moscow State University, edited by P. J. Williams, Cambridge Press, UK.

M. N. Grigoriev, Permafrost Institute, Russian Academy of Sciences, 677018 Yakutsk, Yakutia, Russia.

R. Junker, Leibniz Institute for Applied Geosciences, Geothermal Energy, Stilleweg 2, Niedersachsen, 30655 Hannover, Germany. (ralf.junker@gga-hannover.de)

N. Kaul, University of Bremen, FB5 Geosciences, Postbox 330440, 28334 Bremen, Germany.